



Published in final edited form as:

Cancer Res. 2016 November 15; 76(22): 6723–6734. doi:10.1158/0008-5472.CAN-15-3327.

SRC ONCOGENE INDUCES TROP2 PROTEOLYTIC ACTIVATION VIA CYCLIN D1

Xiaoming Ju^{1,6,*}, Xuanmao Jiao^{1,6,*}, Adam Ertel^{1,6}, Mathew C. Casimiro^{1,6}, Gabriele Di Sante^{1,6}, Shengqiong Deng^{1,6}, Zhiping Li^{1,6}, Agnese Di Rocco^{1,6}, Tingting Zhan^{2,6}, Adam Hawkins^{3,6}, Tanya Stoyanova^{7,^}, Sebastiano Ando⁸, Alessandro Fatatis^{6,9}, Michael P. Lisanti^{4,6,†}, Leonard G. Gomella^{5,6}, Lucia R. Languino^{1,6}, and Richard G. Pestell^{1,4,6,**}

¹Department of Cancer Biology, Thomas Jefferson University, Bluemle Life Sciences Building, 233 South 10th Street, Philadelphia, PA 19107

²Division of Biostatistics, Department of Pharmacology and Experimental Therapeutics, Thomas Jefferson University, Bluemle Life Sciences Building, 233 South 10th Street, Philadelphia, PA 19107

³Medical Oncology, Thomas Jefferson University, Bluemle Life Sciences Building, 233 South 10th Street, Philadelphia, PA 19107

⁴Stem Cell Biology and Regenerative Medicine, Thomas Jefferson University, Bluemle Life Sciences Building, 233 South 10th Street, Philadelphia, PA 19107

⁵Department of Urology, Thomas Jefferson University, Bluemle Life Sciences Building, 233 South 10th Street, Philadelphia, PA 19107

⁶Sidney Kimmel Cancer Center, Thomas Jefferson University, Bluemle Life Sciences Building, 233 South 10th Street, Philadelphia, PA 19107

⁷Department of Microbiology, Immunology, and Molecular Genetics University of California, Los Angeles, CA 90095

⁸Faculty of Pharmacy, Nutrition, and Health Science, University of Calabria, Arcavacata di Rende (CS) 87030

⁹Department of Pharmacology and Physiology and Laboratory Medicine, Drexel University, 245 North 15th St, MS488, 19102

Abstract

Proteomic analysis of castration-resistant prostate cancer demonstrated the enrichment of SRC tyrosine kinase activity in approximately ninety percent of patients. Src is known to induce cyclin

**Corresponding Author: Richard G. Pestell, Department of Cancer Biology, The Sidney Kimmel Cancer Center, Thomas Jefferson University, 233 South 10th Street, Philadelphia, PA 19107, Tel: 215-503-5692; Fax: 215-503-9334, For Reprints: Richard.Pestell@jefferson.edu.

†Equal contribution

^Equal contribution

†Current Address: The Breakthrough Breast Cancer research Unit, University of Manchester, Wilmslow Road, M20, 4BX, Manchester, England, UK.

Current Address: Stanford University, Department of Radiology, 3155 Porter Drive, Palo Alto, CA 94304

Conflict of interest

The authors declare that they have no conflict of interest.

D1, and a cyclin D1-regulated gene expression module predict poor outcome in human prostate cancer. The tumor-associated calcium signal transducer 2 [TACSTD2/Trop2/M1S1] is enriched in the prostate, promoting prostate stem cell self-renewal upon proteolytic activation via a γ -secretase cleavage complex (PS1, PS2) and TACE (ADAM17), which releases the Trop2 intracellular domain (Trop2 ICD). Herein, v-Src transformation of primary murine prostate epithelial cells increased the proportion of prostate cancer stem cells as characterized by gene expression, epitope characteristics and prostatosphere formation. Cyclin D1 was induced by v-Src, and Src kinase induction of Trop2 ICD nuclear accumulation, required cyclin D1. Cyclin D1 induced abundance of the Trop2 proteolytic cleavage activation components (PS2, TACE) and restrained expression of the inhibitory component of the Trop2 proteolytic complex (Numb). Prostate cancer patients with increased nuclear Trop2 ICD and cyclin D1, and reduced Numb, had reduced recurrence-free survival probability (hazard ratio 4.35). Cyclin D1 therefore serves as a transducer of v-Src-mediated induction of Trop2 ICD by enhancing abundance of the Trop2 proteolytic activation complex.

Keywords

Trop2 ICD; Src; cyclin D1; prostate cancer

INTRODUCTION

The *cyclin D1* gene encodes the regulatory subunit of the holoenzyme that phosphorylates and inactivates the retinoblastoma (pRb) protein, promoting G₁/S phase cell cycle entry. Cyclin D1 enhances prostate cellular proliferation *in vivo* and endogenous cyclin D1 maintains prostate cancer cellular proliferation *in vitro* (1). In human prostate cancer, cyclin D1 abundance is increased in many patients and a cyclin D1-regulated gene expression signature predicts poor outcome (1). The abundance of cyclin D1 is induced by activating mutations of Src via transcriptional mechanisms (2). The abundance of cyclin D1 is rate limiting in growth of a variety of tumors *in vivo*, including ErbB2 induced breast cancer (3,4) and a 50% reduction in cyclin D1 abundance in cyclin D1 heterozygote mice is sufficient to reduce the onset and progression of gastrointestinal tumorigenesis induced by the Apc/Min mutation (5).

The Src family of kinases (SFKs) include non-receptor tyrosine kinases with nine homologous members, that encode an SH4 domain governing cytoplasmic membrane association. Src kinase conveys a functional role in both initiation and progression of murine prostate cancer (6,7). Co-expression of wildtype Src and the Androgen Receptor (AR) enhances the formation of murine prostate adenocarcinoma (7). Genomic analysis of human prostate carcinoma demonstrated that mutations of activating tyrosine kinases are rare. However, phosphotyrosine peptide analysis with quantitative mass spectrometry demonstrated increased Src kinase activity in most PCa patients, and >80% of patients are candidates for Src-inhibitor treatment (8). In contrast, very few patients were positive for activated states of receptors for MET, ErbB2, or EGFR, despite their detection in prostate cancer cell lines (8). Given the frequency of Src kinase activation in human prostate cancer,

an enhanced understanding of Src-mediated transformation of prostate epithelium is fundamental to improving PCa patient treatments.

A variety of independent analyses have provided supporting evidence for a role of stem cells in the onset and progression of tumorigenesis (9,10). The tumor-associated calcium signal transducer 2 (Trop2) identifies a subpopulation of prostate cells with stem cell characteristics in both murine and human prostate (11). Trop2 is also highly expressed in the proximal region of the prostate. Trop2 has oncogenic activity (12) demonstrated by chimeric cyclin D1-Trop2 fusions in many cancer types, and silencing the fusion protein inhibits tumor growth (13). The related Trop2 family member, EpCAM, is considered a therapeutic target through regulation of cell-cell adhesion (14-16). Trop2 associates with the $\alpha 5$ integrin subunit, and thereby displaces focal adhesion kinase from focal contacts to promote an invasive phenotype. Consistent with this finding, Trop2 is up-regulated in human prostate cancer (PCa) with extracapsular extension (stages pT3/pT4) as compared to organ-confined (stage pT2) PCa (14-16). Intramembrane proteolysis of Trop2 occurs by the TNF α converting enzyme (TACE) then by γ -secretase. Two cleavage products are generated: the extracellular (ECD) and the intracellular domain (ICD). The Trop2 ICD accumulates in the nucleus, co-localizing with β -catenin to promote prostatic intraepithelial neoplasia (PIN) and self-renewal (17). The molecular mechanisms governing the expression and activation of Trop2 are poorly understood. The current studies were undertaken to investigate the mechanisms governing Trop2 activity in prostate cancer and given the importance of Src kinase, to determine the potential role for Src in Trop2 activity.

MATERIALS AND METHODS

Cell culture, DNA transfection, and luciferase assays

LNCaP cell line was obtained from ATCC, the v-Src PEC and the NeuT-PEC cell lines were previously described (18). Original cells were expanded and stored in the liquid nitrogen at early passage. During the experiments, the morphology of all cell lines was checked under phase contrast microscope routinely. For LNCaP cell line, proliferation and AR abundance in response to DHT stimulation were tested by MTT assay and Western-blot. For v-Src-PEC and NeuT-PEC cell lines, the proliferation in response to Src kinase inhibitor or NeuT inhibitor was tested. V-Src or NeuT expression in these cells was checked by Western-blot for verification. All of the newly revived cells were treated with BM-cyclins (Roche) and the mycoplasma contamination was determined with Hoechst 33258 staining under high magnification fluorescent microscope routinely. DNA transfection and luciferase assays were performed as previously described (1,18). The CBF-Luc and -3,400 cyclin D1-Luc reporter plasmids were previously described (19,20). The Src kinase inhibitor PP1 (4-amino-5-(4-methylphenyl)-7-(t-butyl)pyrazolo-d-3-4-pyrimidine (Calbio Chem) and Dasatinib (BMS-354825, Selleckchem), the CDK inhibitor Abemaciclib (MedChem Express), Palbociclib (Sigma-Aldrich), Ribociclib (Selleckchem) and the EGFR inhibitor Canertinib (Selleckchem) were used at the indicated doses.

Mice, Western-blotting and immunohistochemical staining

Experimental procedures with mice were approved by the ethics committee of Thomas Jefferson University. Mouse ventral prostates were fixed in 4% paraformaldehyde, then used for sectioning and hematoxylin and eosin (H&E) staining. Antibodies used for Western blot analysis and immunohistochemical staining in this study were as follows: anti-cyclin D1, anti-Vinculin, anti-PS1, anti-PS2, anti-TACE (Santa Cruz), and anti-Numb (Cell Signaling), anti-Notch 1 (Millipore 07-1232), anti-p-Src (Upstate 07-020, Tyr 416), anti-Src (Oncogene OP07), anti-Trop2- ICD antibody was from Professor Owen Witte (University of California, Los Angeles).

FACS analysis of stem cells

FACS analysis for prostate cancer stem cells was based on prior publications (1,19,21-23). Before labeling, the cells were blocked with normal mouse IgG in 1:100 dilution for 30 min and then incubated with fluorescein isothiocyanate (FITC) or phycoerythrin (PE)-labeled rat anti mouse Sca-1 (clone E13-161.7, Phamingen) (1/100-1/200), PE-labeled rat anti-mouse CD133 (1:10) (clone MB9-3G8, Miltenyl Biotec), PE/Cy5-labeled rat anti-human/mouse CD44 (1:200) (clone IM7, BioLegend, San Diego), PE/Cy5-labeled rat anti-human/mouse CD49f (1/10) and/or FITC-labeled goat anti mouse Trop2 (FAB1122F, R&D) for 1 h. All experiments were conducted at 4°C. Cell sorting was performed on a FACS Calibur cell sorter (BD Biosciences). The data were analyzed with FlowJo software (Tree Star, Inc., Ashland, OR).

Prostatosphere formation assay

V-Src-PEC cells were plated at a density of 10000 cell/ml in ultra-low attachment Corning cell culture plate and grown in DMEM/F12 with B27, 20 ng ml⁻¹ EGF, 2 ng ml⁻¹ FGF and 4 µg ml⁻¹ heparin. Prostatosphere were collected by gentle centrifugation (800 rpm) after 7–10 days and counted under the microscope using 96-well plate (24).

siRNA transfection and shRNA infection

The transfection of siRNA to cyclin D1 and control siRNA into the v-Src cell line, and the infection of cyclin D1 shRNA into LNCaP cells, were performed as previously described (1). pTRIPZ tet inducible shRNA Vector which use TurboRFP as shRNA expression reporter was from Qiagen, Biotechnology.

Immunofluorescence

Cells were grown in four-well chambers, and slides were fixed with 4% paraformaldehyde in PBS for 20 min at room temperature. The slides were rinsed with PBS and permeated with 0.05% NP-40 in PBS. The primary antibodies were rabbit polyclonal Anti-Trop2-ICD (1/200) and mouse anti-β-catenin (Mouse, Santa Cruz SC-7963, 1/100). The secondary antibodies used were rhodamine red X-conjugated goat anti-rabbit IgG (Jackson ImmunoResearch Laboratories; 1/100) and Alexa Fluor 633-conjugated F(ab')₂ fragment of goat anti-mouse immunoglobulin G (IgG; Molecular Probes, Eugene, OR; 1/250). Fluorescence imaging was acquired with a 40x objective of a Zeiss LSM510/META laser confocal microscope. ImageJ was used to quantify fluorescence intensity of whole cell and

nucleus. 30 cells were measured for each sample and the results were shown as Relative Intensity per μm^2 .

Microarray analysis and comparison with cancer stem cell dataset

Transcript expression profiling was previously performed on the v-Src PEC cell lines along with parental PEC using Affymetrix MoGene 1.0ST microarrays and the microarray data were deposited to GEO (GSE 37428) (18). Genes differentially expressed in the v-Src PEC relative to parental PEC were compared with transcript profiles of CD133⁺ prostate cancer stem cells from a previously published study (25). The detail analysis was described in supplemental methods.

Enrichment analysis of gene ontology biological process terms

The Database for Annotation, Visualization and Integrated Discovery (DAVID) (27) functional annotation tool was used to analyze the genes identified in common between CD133⁺ and v-Src PEC differentially expressed gene lists for enriched Gene Ontology biological process (GOBP) terms (28). GOBP terms were reported at a 10% FDR cutoff and ranked based on gene count for visualization in a bar chart.

Trop2, cyclin D1 and Numb correlation with recurrence of prostate cancer

The TMA was constructed at Thomas Jefferson University Hospital. All patients had undergone radical prostatectomies. Ethical approval was obtained from the Thomas Jefferson University Institutional Ethical Review Board. The detail description was in supplemental methods.

IHC stain was conducted using the cyclin D1 antibody (Thermo Fisher Scientific, RB-010-P, 1:2000), rabbit Trop-2 ICD antibody (Gift from Dr. Owen Witte, dilution 1:400), Numb antibody (Abcam, ab14140, 1:250), Presenilin 2 antibody (Santa Cruz, sc-1456, 1:150) by a DAKO Autostainer Plus equipment with an enzyme labelled biotin-streptavidin system. The slides were scanned on a BLISS system (Bacus Laboratory, North Lombard, IL, USA) and quantified based on the staining intensity and the proportion of cells stained. All comparisons of staining intensities were made at 200X magnification.

Kaplan Meier analysis was used to evaluate the difference in recurrence-free survival associated with high expression versus low expression of Trop2 ICD, cyclin D1 and Numb proteins respectively in the 126 samples which had both a clinical record and IHC staining. The Cox-regression fitting proportional hazards models to censored survival data was used to evaluate the association of all three markers to the risk of recurrence. Stratification was performed recursively. Based on the risk score, patients were assigned to high, medium, low risk groups, the difference in recurrence-free survival was evaluated among the three groups.

Statistical analysis

Comparisons between groups were analyzed by the two-sided t-test. A difference of $P < 0.05$ was considered to be statistically significant. All analyses were done with SPSS 11.5 software. Data are expressed as mean \pm SEM.

RESULTS

Src kinase maintains prostate epithelial cell growth and nuclear tumor-associated calcium signal transducer 2 [TACSTD2/TROP2/MISI] Trop2 ICD translocation

In order to determine the functional significance of Src kinase activity in the maintenance of cellular proliferation, v-Src PEC stable prostate cancer cell lines were analyzed. The addition of the Src inhibitor PP1 reduced cellular proliferation by 20% to 50%, in a dose-dependent manner (Fig. 1A). The Src inhibitor Dasatinib similarly reduced cellular proliferation by 10% ($P<0.05$) to 40% ($P<0.001$) in a dose dependent manner (Fig. 1B). Phospho-Src was down regulated upon treatment with Dasatinib and PP1 (Fig. 1C). Cyclin D1 promotes DNA synthesis of the murine prostate and human prostate cancer cell lines (1). The relative abundance of cyclin D1 was reduced 40% by 25-100 nM Dasatinib (Fig. 1C) associated with a reduction in cellular proliferation. PP1 reduced cyclin D1 abundance by 50% (Fig. 1C). In recent studies Trop2, which is known to be expressed in a subpopulation of prostate basal cells with stem cell characteristics, was shown to correlate with poor prognosis in prostate cancer (11,16,29). Trop2 is activated by RIP (regulated intramembrane proteolysis), a mechanism involved in processing and activation of other transmembrane proteins, including N-cadherin and E-cadherin (30). The nuclear intracellular domain (ICD) of Trop2 is found in human prostate cancer, but not in the adjacent benign tissue (17). In order to determine whether Src kinase activity regulates the relative abundance of Trop2 ICD, Western blot analysis was conducted with an ICD-specific antibody. The relative abundance of Trop2 ICD was reduced 50% in the presence of the Src kinase inhibitors, Dasatinib and PP1 (Fig. 1C). In order to examine the kinetics with which Src kinase inhibition by Dasatinib reduced the abundance of the Trop2 ICD, a time course was conducted. Cyclin D1 levels were reduced >50% by 24 hrs, and >90% by 48 hrs. The reduction in Trop2 ICD abundance was reduced 50% at 48 hrs (Supplemental Fig. 1).

v-Src induces gene expression of prostate cancer stem cell epitopes

In order to examine the molecular signaling pathways activated upon v-Src transformation of prostate epithelial cells, gene expression profiling was conducted to compare v-Src transformed PEC and parental PEC. Experiments were conducted on 3 separate PEC-Src lines (Fig. 2A). In previous studies CD133⁺ cells were considered enriched for prostate cancer stem cells (31,32). A correlative analysis was conducted examining the genes that were differentially expressed between the CD133⁺ vs. CD133⁻ prostate cancer cells (25). We therefore compared the genes enriched by v-Src in PEC with the genes expressed in CD133⁺ prostate cells. The relative abundance of genes in the CD133⁺ prostate cancer stem cell signature is shown in Figure 2A (left hand panel). The genes differentially expressed within v-Src prostate cancer cell lines, relative to non-transformed parental prostate epithelial cells, are shown as the differentially expressed genes to the right (18). A substantial overlap was seen between the genes enriched in CD133⁺ prostate cells when compared with genes regulated by v-Src. Genes induced within CD133⁺ cells were also induced by v-Src, and genes repressed by CD133⁺ were repressed by v-Src (Fig. 2A). The P-value for the degree of similarity of the CD133⁺ stem cell signature with v-Src regulated genes was significant ($P=2.148 \times 10^{-10}$) (Fig. 2A).

77 genes regulated by v-Src (77/466, ~17%) were regulated by CD133⁺ in a common manner ($P=5.52 \times 10^{-14}$) (Fig. 2B). These studies suggest an enrichment of Src regulated genes amongst the CD133 enriched genes. Go Terms were used to identify gene pathways regulated upon v-Src transformation of PEC. Additional pathways enriched upon v-Src transformation of PEC, included “cell cycle, DNA damage repair, DNA metabolic process and chromosomal organization” (Fig. 2C). In order to determine whether CD133⁺ cells were enriched for Src kinase activity, the oncogene transformed PEC were FACS sorted for CD133 and then characterized for Src activity using the antibody directed to activated Src (Src^P Tyr 416) (Fig. 2D). CD133⁺ cells were enriched 3-fold for Src^P Tyr 416 compared with CD133⁻ cells (Fig. 2E).

v-Src transformation induces epitope markers of prostate cancer stem cells

Prostatosphere formation assays, a surrogate measure of prostate cancer stem cells, were performed on the v-Src PEC cell. Approximately 3.6 out of 1,000 cells formed prostatospheres in v-Src PEC, while in parental PEC cells only 1 out of 1000 formed (Fig. 3A). The v-Src-PEC line derived prostatospheres were consistently larger than the non-transformed, and only the v-Src-PEC lines gave rise to secondary prostatospheres (Fig. 3A). Treatment with the Src kinase inhibitors Dasatinib or PP1 reduced the number (Fig. 3B) but not the size of the prostatospheres.

In view of the finding that v-Src transformation induced expression of genes associated with CD133⁺, a prostate stem cell marker, we examine further the association of v-Src transformation with the expression of prostatic cancer stem cell epitopes. Fluorescence activated cell sorting (FACS) was conducted for the relative proportion of other epitope markers of prostate cancer stem cells. v-Src transformation of prostate epithelium was associated with an approximately 8-fold increase of Sca1^{high} cells (Fig. 3B). Similarly, the proportion of CD44⁺/CD133⁺ cells was increased 6-fold (Fig. 3C). The proportion of CD49f⁺ Sca1⁺ Trop2⁺ cells was increased 2.4-fold in v-Src transformed PEC cells compared to parental PEC (Fig. 3D).

Src kinase activity induces nuclear Trop2 ICD abundance in cultured prostate cancer cells and *in vivo*

Although the total Trop2 ICD abundance was reduced by Src kinase inhibitor, the nuclear pool of Trop2-ICD is considered to be the biologically active moiety, therefore we next sought to determine whether Src kinase governs the abundance of nuclear Trop2 ICD. Comparison was made between parental and v-Src transformed PEC by immunostaining for Trop2-ICD (red), β -catenin (green) and nucleus (DAPI, blue) (Fig. 4A). The relative abundance of nuclear Trop2 ICD was enhanced 4-fold upon v-Src transformation (Fig. 4A). The addition of the Src inhibitor, either 100 nM Dasatinib or 10 μ M PP1, reduced nuclear Trop2 ICD abundance by ~40% (Fig. 4D). In contrast β -catenin immunostaining was not significantly reduced by Dasatinib.

The v-Src PEC lines were derived from FVB murine prostate epithelium and can therefore be reintroduced into immune competent FVB mice (18). In view of the importance of the immune system in the onset and progression of prostate cancer, we examined the abundance

of the Trop2 ICD in v-Src tumors implanted into immune competent mice *in vivo*. The presence of nuclear Trop2 ICD was demonstrated in the v-Src prostate tumors *in vivo* (Fig. 4E). The relative staining of the Trop2 ICD in the v-Src prostate tumors was increased 2-fold compared to the non-transformed murine prostate gland (Fig. 4F). The induction of Trop2 abundance assessed by Western blot was increased ~10-fold in a series of v-Src tumors derived after implantation in FVB mice (Fig. 4G). RNA extracted from v-Src tumor and normal ventral prostate tissues was assessed by microarray analysis. The relative mRNA abundance of Trop2 was induced 3.5-fold. We examined the abundance of several other genes associated with the prostate cancer stem cell signature (33). Notch1 was induced 3.5-fold. CD44 mRNA was induced more than 5-fold (Fig. 4H), CD44 is a cell adhesion glycoprotein that participates in presentation of cytokines and associates with stem cell functions (34). The abundance of Wnt7A was induced 50% (Fig. 4H), consistent with recent studies suggesting heterotypic signaling from the interstitium maintains prostate cancer progression (35).

Cyclin D1 is required for Trop2 ICD nuclear accumulation

Previous studies in human breast cancer cells demonstrated that cyclin D1 enhances Notch1 activity through inducing γ -secretase activity (19). The γ -secretase cleavage complex components presenilin1 (PS1) and presenilin2 (PS2) contribute to the γ -secretase activity governing Trop2 cleavage (17). We therefore examined the potential importance of cyclin D1 in the induction of the Trop2 ICD. In order to determine the mechanism by which Src induces cyclin D1 abundance, we first examined the relative abundance of cyclin D1 in v-Src vs. parental PEC. Cyclin D1 mRNA was induced 2-fold by v-Src transformation (18). The -3,400 bp cyclin D1 promoter fragment linked to a luciferase reporter gene was induced 2-fold by v-Src (Fig. 5A) and reduced 80% by Dasatinib in v-Src PEC (Fig. 5B). Immunohistochemical staining for Trop2 ICD was conducted in *cyclin D1^{+/+}* and *cyclin D1^{-/-}* mouse prostate. We observed a 4-fold decrease of nuclear Trop2 ICD in cyclin D1 knockout prostates when compare to normal wild type prostate (Fig. 5C). In order to determine whether cyclin D1-mediated induction of Trop2 ICD nuclear abundance is regulated in transformed prostate cancer cells, a cyclin D1 shRNA linked to a tet-inducible red fluorescent protein, (RFP) was introduced into the LNCaP prostate cancer epithelial cell line (Fig. 5D). The addition of doxocycline induced the expression system and thereby RFP (Fig. 5D). Western blot demonstrated cyclin D1 shRNA reduced the relative abundance of cyclin D1 by >50%, associated with a reduction in Trop2 ICD by ~ 50% (Fig. 5E). Vinculin, used as a control for normalization of protein abundance was unchanged (Fig. 5E). Immunofluorescence staining for nuclear Trop2 in LNCaP cells treated with cyclin D1 shRNA demonstrated the reduction in nuclear Trop2 ICD upon induction of cyclin D1 shRNA (Fig. 5F, G). CBF-1 (C-promoter binding factor-1), the mammalian homologue of Suppressor of Hairless (*Drosophila*) and CSL protein in *C. elegans*, also known as RBP-JK, is activated by the Trop2 ICD. As our studies showed v-Src enhanced Trop2 cleavage, we determined whether CBF activity was maintained by v-Src kinase activity in prostate cancer cells. CBF activity was assessed using a synthetic CBF luc reporter in v-Src PEC line. The Src kinase inhibitors Dasatinib and PP1 reduced CBF activity in a dose-dependent manner (Fig. 5H). Cyclin D1 siRNA reduced CBF (CBF8luc) activity ~ 2-fold in v-Src PEC line (Fig. 5I).

Cyclin D1 induces expression of the Trop2 cleavage complex

Intramembrane proteolysis of Trop2 occurs via a γ -secretase cleavage complex (which includes PS1 and PS2) and TACE (ADAM17). In order to determine the mechanism by which cyclin D1 enhances Trop2 ICD accumulation, we considered that cyclin D1 may increase the abundance of the Trop2 cleavage complex. Immunohistochemical staining of *cyclin D1^{+/+}* and *cyclin D1^{-/-}* mouse prostate glands was conducted to examine the abundance of the components regulating Trop2 ICD abundance. TACE and PS2 are the key inducers of Trop2 cleavage (17). Therefore we examined TACE and PS2 in *cyclin D1^{+/+}* and *cyclin D1^{-/-}* prostate (Fig. 6A). The deletion of the *cyclin D1* gene reduced TACE and PS2 abundance in the prostate by 50% (Fig. 6B, C). Previous studies had demonstrated that cyclin D1 represses Numb to thereby induce Notch1 activity in breast cancer cells (19). As Notch can also activate CBF, we considered the possibility that endogenous cyclin D1 may induce CBF through repression of Numb in prostate epithelium. Consistent with prior findings in the mammary gland, we found *cyclin D1* gene deletion enhanced Numb abundance in the prostate *in vivo* (Fig. 6D). In order to determine whether the mRNA levels of the Trop2 cleavage complex were induced by cyclin D1, mRNA levels of the Trop2 proteolytic cleavage components were assessed in prostate tissues of *cyclin D1^{+/+}* and *cyclin D1^{-/-}* mice by RT-PCR (Fig. 6E). Cyclin D1 reduced Numb and increased PS2 and TACE (Fig. 6E). In order to determine whether cyclin D1 maintains expression of the Trop2 cleavage complex in transformed prostate cells, Western Blot was conducted on cyclin D1 transduced v-Src PEC. Commensurate with the ~50% reduction in cyclin D1 abundance, Trop2 ICD abundance was reduced ~50%, PS2 was reduced ~50%, associated with the reduction of TACE (ADAM17) (Fig. 6F).

Cyclin D1 is known to convey kinase-dependent and kinase-independent functions. In order to determine whether the induction of Trop2 by cyclin D1 was kinase dependent we examined the effect of inhibiting cyclin D1/cdk activity using the cdk inhibitors Abemaciclib, Palbociclib and Ribociclib. The cdk inhibitors reduced pRb^p at 24 hrs, and reduced Trop2 ICD abundance at 48 and 72 hrs. At 48 hrs the reduction in Trop2 ICD was 10% with Abemaciclib (x mM), whereas Palbociclib (>60%) and Ribociclib (>60%) was more substantial.

In order to examine further the specificity of the effect mediated by oncogenic Src we examined the possibility that growth factor signaling via the EGFR may induce Trop2 ICD. We therefore tested the EGFR antagonist Canertinib. Canertinib is a 3-chloro 4-fluoro 4-anilinoquinazoline compound. It is a low-molecular-weight irreversible pan-EGFR family TKI and has been shown to inhibit cell proliferation via restraint of ERK/MAPK in a number of different cell types. Canertinib treatment of the PEC-Src inhibited cell proliferation (Supplemental Fig. 2A). Canertinib treatment of the PEC-Src did not affect levels of Trop2 ICD, and did not affect cyclin D1 levels. These findings suggest that dissociable pathways conduct selective signaling to Trop2-ICD abundance. Together these studies demonstrate that v-Src induces cyclin D1, and that cyclin D1 induces expression of components of the Trop2 cleavage complex, directly through increasing PS2 and TACE, and indirectly through reducing Numb, thereby enhancing the abundance of the Trop2 ICD, and CBF activity in prostate cancer cells (Supplemental Fig. 3).

Cyclin D1, Trop2 ICD and Numb predict outcome of prostate cancer patients

In order to determine whether the abundance of cyclin D1, Trop2 ICD, PS2 and Numb correlate with outcome in human prostate cancer, an annotated Tissue Microarray (TMA) of patients with prostate cancer was analyzed. IHC staining was conducted of a 126 prostate cancer patient TMA. The expression of cyclin D1, Trop2 ICD, PS2 and Numb was quantified (Supplemental Fig. 4). Kaplan Meier analysis was used to evaluate the difference in recurrence-free survival associated with high expression versus low expression of cyclin D1, Trop2 ICD, PS2 and Numb. Survival probability of cyclin D1 high expression group was ~60%, while low expression group is more than 90%. The difference was significant ($P=0.049$) (Fig. 7A). The survival probability of Trop2 ICD high expression group was ~25%, which was significantly increased to 73% in the low expression group ($P=0.008$) (Fig. 7B). The change in survival probability between PS2 groups was not significant (Fig. 7C). In the low Numb expression group the survival probability was reduced to 0% compared to 72% for the high expression group ($P<0.001$) (Fig. 7D). These three target genes were combined and recurrence-free survival analysis was conducted. Using the Cox model based on the risk score determined by recursive partitioning with the predictors, cyclin D1, Numb and Trop2, patients were assigned to high, medium, low recurrence risk groups, and the recurrence free survival curves of different groups and hazard ratios between the groups were analyzed. Compared to the low risk group, the hazard ratio for survival was increase 3- fold in the medium risk group and 4.3- fold in the high risk group ($P<0.001$) (Fig. 7E).

DISCUSSION

Src kinase is increased in ~80% of human prostate cancers (8). The current studies provide several lines of evidence that v-Src transformation of prostate epithelial cells enriches for prostate cancer stem cell. Firstly, v-Src transformation induced expression of genes identified in prostate cancer stem cells. Genes associated with the prostate cancer stem cell signature (33), included Notch1 which was induced 3.5-fold. CD44 mRNA, which encodes a cell adhesion glycoprotein that participates in presentation of cytokines and associates with stem cell functions (34), was induced more than 5-fold (Fig. 4H). The abundance of Wnt7A was induced 50% consistent with recent studies suggesting heterotypic signaling from the interstitium maintains prostate cancer progression (35). CD133⁺ cells are enriched for cancer stem cells repopulating from prostate cancer (36). Together with $\alpha 2\beta 1$ integrin, CD133 is used to enrich for stem cells that have increased proliferation potential and undergo full prostatic differentiation *in vivo* (37-39). Approximately 17% of genes enriched in the CD133 population were also induced by oncogenic Src transformation. Secondly, v-Src induced the abundance of the epitopes characteristic of prostate cancer stem cells. Thirdly, v-Src induced prostatosphere formation and, Src kinase inhibitors reduced the number of prostatospheres. Fourthly, the abundance of the Trop2 ICD which is known to promote stem cell expansion (17,19), was enhanced by Src kinase activity.

In the current studies, cyclin D1 was required for v-Src induced Trop2 ICD accumulation. The TNF α converting enzyme (TACE), and γ -secretase, both participate in Trop2 ICD accumulation. TACE mediates the initial proteolysis and ectodomain shedding, followed by

intramembrane proteolysis carried out by the γ -secretase complex. Herein, endogenous cyclin D1 was shown to enhance expression of the Trop2 cleavage complex by increasing the abundance of TACE (ADAM17) and PS2. TACE is a member of the ADAM family of proteases. Our prior studies demonstrated that endogenous cyclin D1 maintains ADAM protease expression in the mammary gland (40). In the current studies, cyclin D1 induced the abundance of TACE in the normal prostate gland. In prostate epithelial cells in culture and in transformed prostate cancer cells, cyclin D1 also induced expression of PS2, the catalytic subunit of the γ -secretase complex that conducts the sequential intramembrane proteolysis of Trop2 (40). Thus, consistent with the finding in the mammary gland *in vivo*, in which cyclin D1 induced the ADAM proteases, the current studies demonstrate cyclin D1 induces expression of ADAM17 proteases (TACE) in the prostate *in vivo*.

In the current studies endogenous cyclin D1 augmented CBF activity in a Src-kinase-dependent manner. Trop2 and Notch augment activity of the transcription factor CBF-1 (suppressor of hairless, LAG1, also known as RBP-RJ) (41) and LEF-1. Notch activity is restrained by endogenous Numb. In the current studies endogenous cyclin D1 repressed Numb in PCa cells. These findings are consistent with prior studies in breast cancer epithelial cells in which cyclin D1 augmented ErbB2-induced Notch1 activity, through repression of Numb (19). These prior studies demonstrated the induction of Notch signaling by cyclin D1 (19). Using cyclin D1 knockout mice, it was demonstrated that γ -secretase cleavage of Notch1 was enhanced by endogenous cyclin D1 (19). In a reciprocal feedback, Notch is known to induce cyclin D1 expression and cyclin D1 is required for Notch induced transformation (42), consistent with findings that Notch1 and cyclin D1 expression correlate during embryogenesis (42).

The current studies demonstrated that a reduction in Numb, an increase in Trop2 ICD and an increase in cyclin D1 abundance, each predict poor outcome in patients with prostate cancer. When combined, these three genes assigned to high, medium, or low recurrence risk groups, gave a high risk group with a hazards ratio 4.35 times greater than the low risk group. Although cyclin D1 protein is overexpressed in a subset of prostate cancers, correlating with poor outcome, it is the cyclin D1-mediated gene expression signature that provides additional prognostic value to the Gleason Score (1,43). The current studies are consistent with a model in which the molecular targets of cyclin D1-mediated signaling in the prostate are important predictors of poor outcome in prostate cancer.

Supplementary Material

Refer to Web version on PubMed Central for supplementary material.

Acknowledgments

Financial support

This work was supported in part by NIH grants R01CA070896, R01CA075503, R01CA132115, R01CA107382, R01CA086072 (R.G. Pestell), R01CA109874 (L.R. Languino) the Sidney Kimmel Cancer Center NIH Cancer Center Core grant P30CA056036 (R.G. Pestell), generous grants from the Dr. Ralph and Marian C. Falk Medical Research Trust (R.G. Pestell) a grant from Pennsylvania Department of Health (R.G. Pestell). M.P. Lisanti and his laboratory were supported via the resources of Thomas Jefferson University.

References

1. Ju X, Casimiro MC, Gormley M, Meng H, Jiao X, Katiyar S, et al. Identification of a cyclin D1 network in prostate cancer that antagonizes epithelial-mesenchymal restraint. *Cancer Res.* 2014; 74:508–19. [PubMed: 24282282]
2. Lee RJ, Albanese C, Stenger RJ, Watanabe G, Inghirami G, Haines GK 3rd, et al. pp60(v-src) induction of cyclin D1 requires collaborative interactions between the extracellular signal-regulated kinase, p38, and Jun kinase pathways. A role for cAMP response element-binding protein and activating transcription factor-2 in pp60(v-src) signaling in breast cancer cells. *J Biol Chem.* 1999; 274:7341–50. [PubMed: 10066798]
3. Lee RJ, Albanese C, Fu M, D'Amico M, Lin B, Watanabe G, et al. Cyclin D1 is required for transformation by activated Neu and is induced through an E2F-dependent signaling pathway. *Molecular and cellular biology.* 2000; 20:672–83. [PubMed: 10611246]
4. Yu Q, Geng Y, Sicinski P. Specific protection against breast cancers by cyclin D1 ablation. *Nature.* 2001; 411:1017–21. [PubMed: 11429595]
5. Hult J, Wang C, Li Z, Albanese C, Rao M, Di Vizio D, et al. Cyclin D1 genetic heterozygosity regulates colonic epithelial cell differentiation and tumor number in ApcMin mice. *Molecular and cellular biology.* 2004; 24:7598–611. [PubMed: 15314168]
6. Kraus S, Gioeli D, Vomastek T, Gordon V, Weber MJ. Receptor for activated C kinase 1 (RACK1) and Src regulate the tyrosine phosphorylation and function of the androgen receptor. *Cancer Res.* 2006; 66:11047–54. [PubMed: 17108144]
7. Cai H, Babic I, Wei X, Huang J, Witte ON. Invasive prostate carcinoma driven by c-Src and androgen receptor synergy. *Cancer Res.* 2011; 71:862–72. [PubMed: 21135112]
8. Drake JM, Graham NA, Lee JK, Stoyanova T, Faltermeier CM, Sud S, et al. Metastatic castration-resistant prostate cancer reveals intrapatient similarity and interpatient heterogeneity of therapeutic kinase targets. *Proceedings of the National Academy of Sciences of the United States of America.* 2013; 110:E4762–9. [PubMed: 24248375]
9. Yu Z, Pestell TG, Lisanti MP, Pestell RG. Cancer stem cells. *The international journal of biochemistry & cell biology.* 2012; 44:2144–51. [PubMed: 22981632]
10. Korkaya H, Liu S, Wicha MS. Breast cancer stem cells, cytokine networks, and the tumor microenvironment. *The Journal of clinical investigation.* 2011; 121:3804–9. [PubMed: 21965337]
11. Goldstein AS, Lawson DA, Cheng D, Sun W, Garraway IP, Witte ON. Trop2 identifies a subpopulation of murine and human prostate basal cells with stem cell characteristics. *Proc Natl Acad Sci U S A.* 2008; 105:20882–7. [PubMed: 19088204]
12. Shvartsur A, Bonavida B. Trop2 and its overexpression in cancers: regulation and clinical/therapeutic implications. *Genes & cancer.* 2015; 6:84–105. [PubMed: 26000093]
13. Guerra E, Trerotola M, Dell'Arciprete R, Bonasera V, Palombo B, El-Sewedy T, et al. A bicistronic CYCLIN D1-TROP2 mRNA chimera demonstrates a novel oncogenic mechanism in human cancer. *Cancer Res.* 2008; 68:8113–21. [PubMed: 18829570]
14. Dalerba P, Dylla SJ, Park IK, Liu R, Wang X, Cho RW, et al. Phenotypic characterization of human colorectal cancer stem cells. *Proc Natl Acad Sci U S A.* 2007; 104:10158–63. [PubMed: 17548814]
15. Baeuerle PA, Gires O. EpCAM (CD326) finding its role in cancer. *Br J Cancer.* 2007; 96:417–23. [PubMed: 17211480]
16. Trerotola M, Ganguly KK, Fazli L, Fedele C, Lu H, Dutta A, et al. Trop-2 is up-regulated in invasive prostate cancer and displaces FAK from focal contacts. *Oncotarget.* 2015; 6:14318–28. [PubMed: 26015409]
17. Stoyanova T, Goldstein AS, Cai H, Drake JM, Huang J, Witte ON. Regulated proteolysis of Trop2 drives epithelial hyperplasia and stem cell self-renewal via beta-catenin signaling. *Genes Dev.* 2012; 26:2271–85. [PubMed: 23070813]
18. Ju X, Ertel A, Casimiro MC, Yu Z, Meng H, McCue PA, et al. Novel oncogene-induced metastatic prostate cancer cell lines define human prostate cancer progression signatures. *Cancer Res.* 2013; 73:978–89. [PubMed: 23204233]

19. Lindsay J, Jiao X, Sakamaki T, Casimiro MC, Shirley LA, Tran TH, et al. ErbB2 induces Notch1 activity and function in breast cancer cells. *Clin Transl Sci*. 2008; 1:107–15. [PubMed: 20443831]
20. Rao M, Casimiro MC, Lisanti MP, D'Amico M, Wang C, Shirley LA, et al. Inhibition of cyclin D1 gene transcription by Brg-1. *Cell cycle*. 2008; 7:647–55. [PubMed: 18239461]
21. Jiao X, Katiyar S, Willmarth NE, Liu M, Ma X, Flomenberg N, et al. c-Jun induces mammary epithelial cellular invasion and breast cancer stem cell expansion. *J Biol Chem*. 2010; 285:8218–26. [PubMed: 20053993]
22. Liu M, Casimiro MC, Wang C, Shirley LA, Jiao X, Katiyar S, et al. p21CIP1 attenuates Ras- and c-Myc-dependent breast tumor epithelial mesenchymal transition and cancer stem cell-like gene expression in vivo. *Proc Natl Acad Sci U S A*. 2009; 106:19035–9. [PubMed: 19858489]
23. Wu K, Jiao X, Li Z, Katiyar S, Casimiro MC, Yang W, et al. Cell fate determination factor Dachshund reprograms breast cancer stem cell function. *J Biol Chem*. 2011; 286:2132–42. [PubMed: 20937839]
24. Jiao X, Rizvanov AA, Cristofanilli M, Miftakhova RR, Pestell RG. Breast Cancer Stem Cell Isolation. *Methods in molecular biology*. 2016; 1406:121–35. [PubMed: 26820950]
25. Birnie R, Bryce SD, Roome C, Dussupt V, Droop A, Lang SH, et al. Gene expression profiling of human prostate cancer stem cells reveals a pro-inflammatory phenotype and the importance of extracellular matrix interactions. *Genome Biol*. 2008; 9:R83. [PubMed: 18492237]
26. Irizarry RA, Bolstad BM, Collin F, Cope LM, Hobbs B, Speed TP. Summaries of Affymetrix GeneChip probe level data. *Nucleic Acids Res*. 2003; 31:e15. [PubMed: 12582260]
27. Dennis G Jr, Sherman BT, Hosack DA, Yang J, Gao W, Lane HC, et al. DAVID: Database for Annotation, Visualization, and Integrated Discovery. *Genome Biol*. 2003; 4:P3. [PubMed: 12734009]
28. Ashburner M, Ball CA, Blake JA, Botstein D, Butler H, Cherry JM, et al. Gene ontology: tool for the unification of biology. The Gene Ontology Consortium. *Nat Genet*. 2000; 25:25–9. [PubMed: 10802651]
29. Goldstein AS, Huang J, Guo C, Garraway IP, Witte ON. Identification of a cell of origin for human prostate cancer. *Science*. 2010; 329:568–71. [PubMed: 20671189]
30. Brown MS, Ye J, Rawson RB, Goldstein JL. Regulated intramembrane proteolysis: a control mechanism conserved from bacteria to humans. *Cell*. 2000; 100:391–8. [PubMed: 10693756]
31. Pellacani D, Oldridge EE, Collins AT, Maitland NJ. Proliferin-1 (CD133) Expression in the Prostate and Prostate Cancer: A Marker for Quiescent Stem Cells. *Advances in experimental medicine and biology*. 2013; 777:167–84. [PubMed: 23161082]
32. Vander Griend DJ, Karthaus WL, Dalrymple S, Meeker A, DeMarzo AM, Isaacs JT. The role of CD133 in normal human prostate stem cells and malignant cancer-initiating cells. *Cancer Res*. 2008; 68:9703–11. [PubMed: 19047148]
33. Smith BA, Sokolov A, Uzunangelov V, Baertsch R, Newton Y, Graim K, et al. A basal stem cell signature identifies aggressive prostate cancer phenotypes. *Proc Natl Acad Sci U S A*. 2015; 112:E6544–52. [PubMed: 26460041]
34. Bourguignon LY, Peyrollier K, Xia W, Gilad E. Hyaluronan-CD44 interaction activates stem cell marker Nanog, Stat-3-mediated MDR1 gene expression, and ankyrin-regulated multidrug efflux in breast and ovarian tumor cells. *J Biol Chem*. 2008; 283:17635–51. [PubMed: 18441325]
35. Goldstein AS, Witte ON. Does the microenvironment influence the cell types of origin for prostate cancer? *Genes Dev*. 2013; 27:1539–44. [PubMed: 23873937]
36. Collins AT, Berry PA, Hyde C, Stower MJ, Maitland NJ. Prospective identification of tumorigenic prostate cancer stem cells. *Cancer Res*. 2005; 65:10946–51. [PubMed: 16322242]
37. Collins AT, Habib FK, Maitland NJ, Neal DE. Identification and isolation of human prostate epithelial stem cells based on alpha(2)beta(1)-integrin expression. *J Cell Sci*. 2001; 114:3865–72. [PubMed: 11719553]
38. Richardson GD, Robson CN, Lang SH, Neal DE, Maitland NJ, Collins AT. CD133, a novel marker for human prostatic epithelial stem cells. *J Cell Sci*. 2004; 117:3539–45. [PubMed: 15226377]
39. Berry PA, Maitland NJ, Collins AT. Androgen receptor signalling in prostate: effects of stromal factors on normal and cancer stem cells. *Molecular and cellular endocrinology*. 2008; 288:30–7. [PubMed: 18403105]

40. Casimiro MC, Wang C, Li Z, Di Sante G, Willmart NE, Addya S, et al. Cyclin D1 determines estrogen signaling in the mammary gland in vivo. *Mol Endocrinol.* 2013; 27:1415–28. [PubMed: 23864650]
41. Eric J, Allenspach IM, Jon C Aster, Warren S Pear. Notch Signaling in Cancer. *Cancer Biology & Therapy.* 2002; 1:466–76. [PubMed: 12496471]
42. Mark Stahl CG, Shaolin Shi, Richard G Pestell, Pamela Stanley. Notch1-Induced Transformation of RKE-1 Cells Requires Up-regulation of Cyclin D1. *Cancer Research.* 2006; 66:7562–70. [PubMed: 16885355]
43. Ding Z, Wu CJ, Chu GC, Xiao Y, Ho D, Zhang J, et al. SMAD4-dependent barrier constrains prostate cancer growth and metastatic progression. *Nature.* 2011; 470:269–73. [PubMed: 21289624]

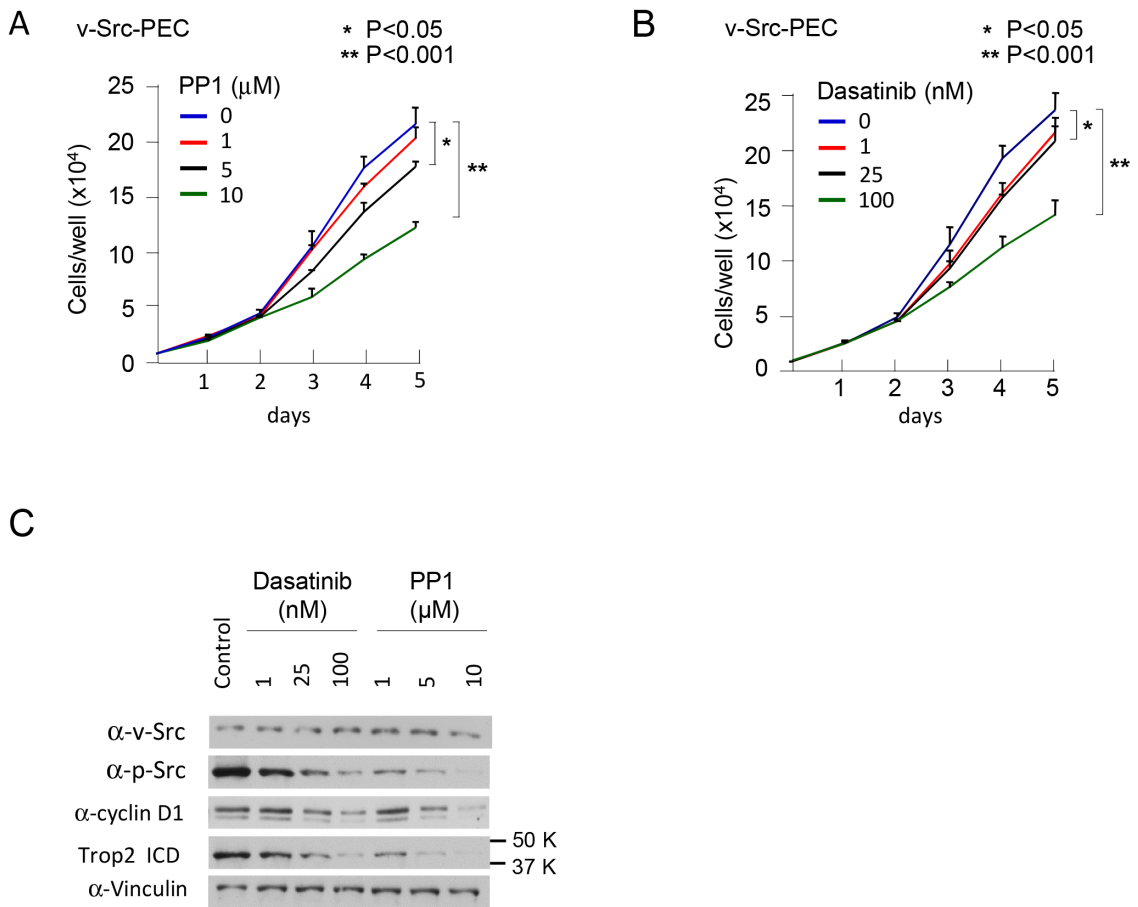


Figure 1. Src kinase activity promotes v-Src prostate cancer cell line proliferation

(A) Cellular proliferation assays were conducted by cell counting in the presence of either control or Src inhibitor (PP1), or (B) the Src inhibitor Dasatinib with doses as indicated. (C) Western blot analysis of v-Src prostate cancer cell lines treated with the Src inhibitors Dasatinib or PP1. The antibodies were directed to the proteins as indicated.

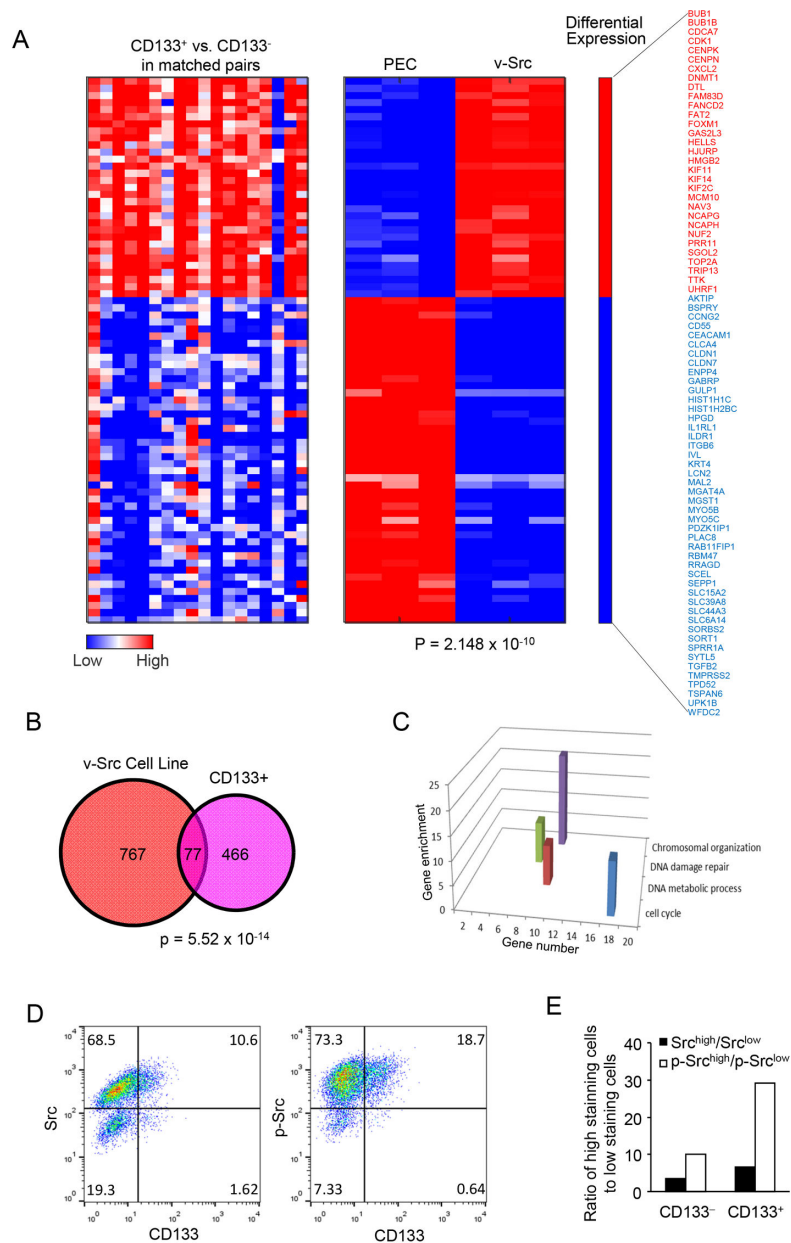


Figure 2. Microarray analysis of v-Src PEC cells compared to the gene expression profile enriched in CD133⁺ prostate cancer cells

(A vs. B) Heatmaps show the intersection of differentially expressed genes from paired CD133⁺ vs CD133⁻ sample data (25) (left) and genes that are differentially expressed in the v-Src oncogene cell line (right). A Venn diagram represents the degree of overlap among differentially expressed genes in CD133⁺ cells and v-Src, 767 genes specific to v-Src cell lines, and 466 genes specific to the CD133⁺ cells, with a 77-gene overlap. (C) Gene Ontology biological process was analyzed for the overlapping 77 genes, the induced functional pathways were shown with the fold enrichment and the number of gene for each GO term. (D) FACS analysis on NeuT-transformed PEC cells showed that there were less CD133⁺ cells with lower Src activity than CD133⁻ cells.

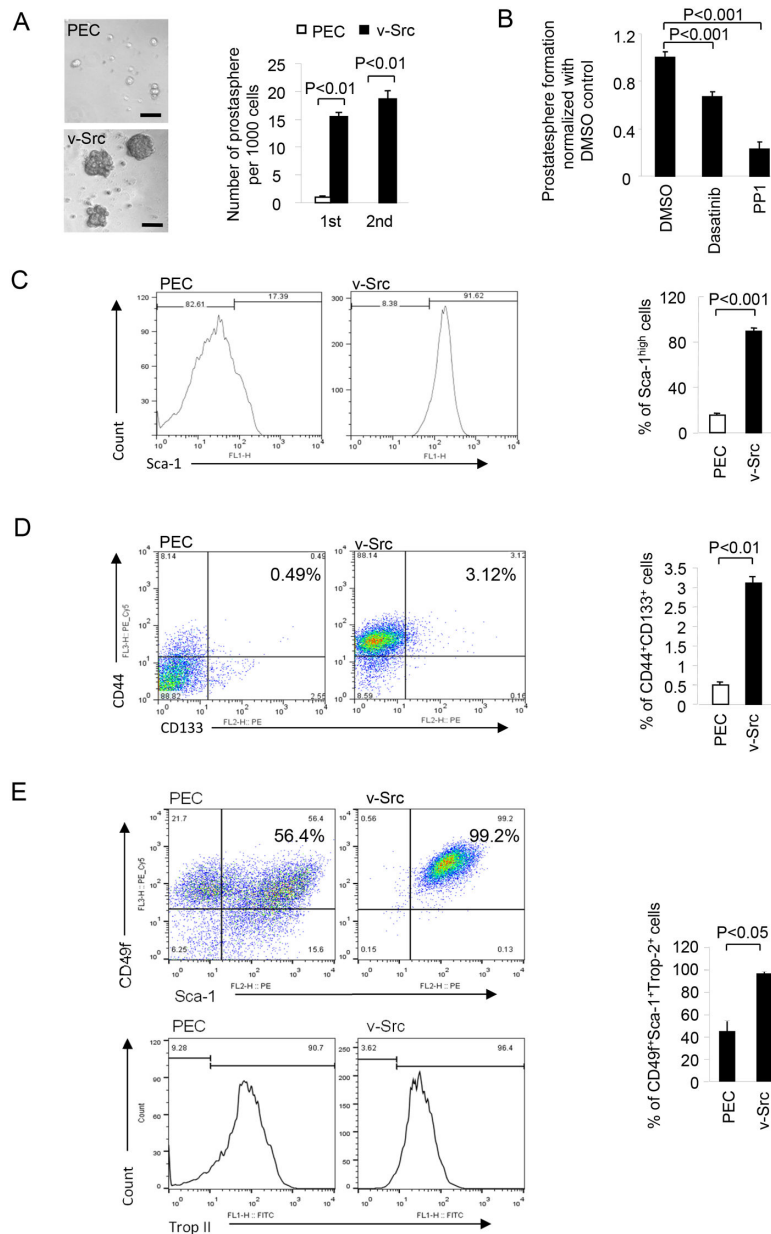


Figure 3. v-Src transformation induces epitope markers of prostate cancer stem cells
 (A) 1st and 2nd generation of prostatesphere formation assay was performed on the v-Src transformed PEC cells. (B) The effects of Src-inhibitor Dasatinib and PP1 on prostatesphere formation of v-Src transformed PEC cells. The relative abundance of prostate cancer stem cell markers were assessed by FACS analysis, including (C) Sca1^{high} cells increased 8-fold in v-Src PEC cells, (D) CD44⁺ CD133⁺ cells increased 6-fold and (E) CD49⁺ Sca1⁺ Trop2⁺ cells increased 2.4-fold compared to parental PEC.

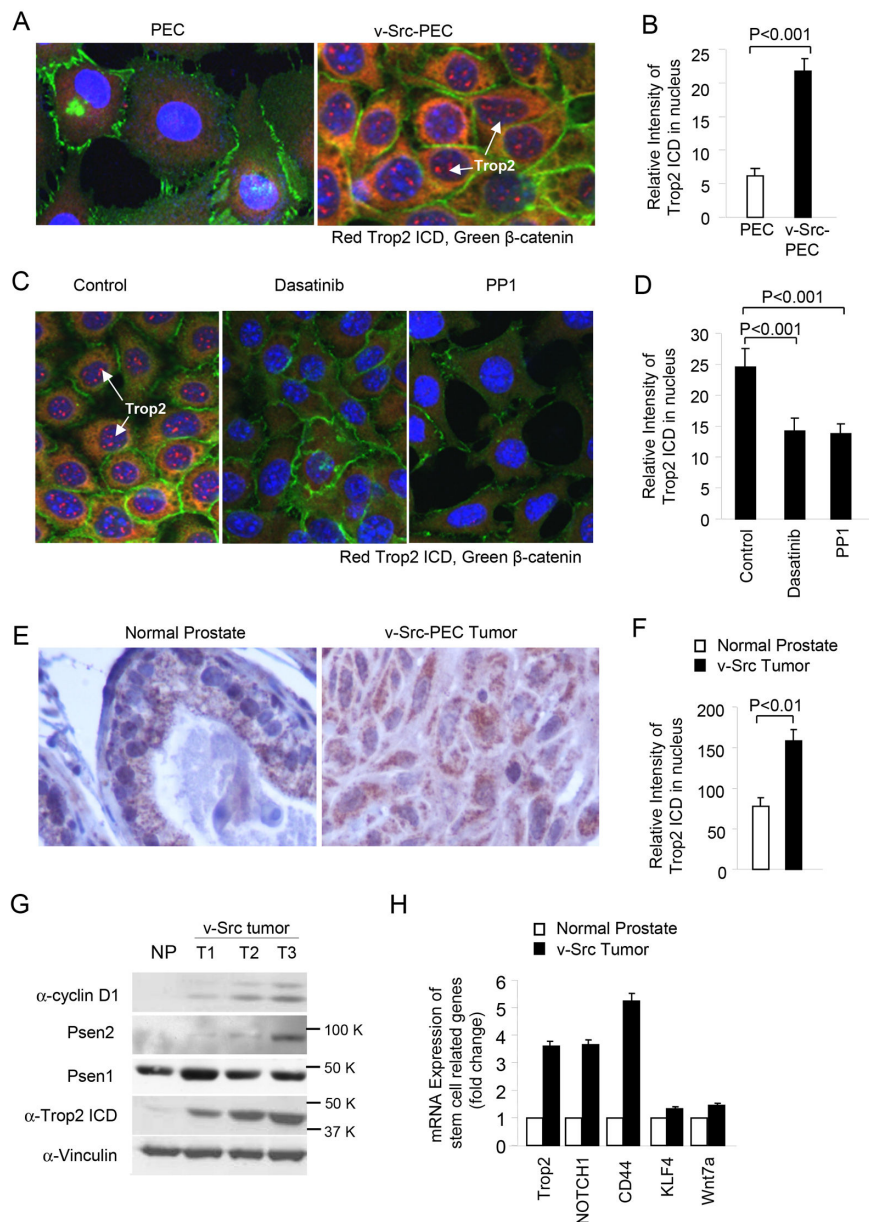


Figure 4. v-Src transformation enhances nuclear Trop2 ICD expression *in vitro* and *in vivo*
 (A) Immunofluorescence staining for Trop2 ICD of v-Src transformed cells vs. parental PEC cells, and (B) the intensity of nuclear Trop2 ICD was quantified. (C) The treatment of v-Src PEC lines with the Src inhibitors PP1 and Dasatinib shows the reduction in nuclear Trop2 staining upon treatment with Src kinase inhibitor, the relative intensity of Trop2 ICD (D). (E) The presence of nuclear Trop2 ICD was shown in the normal ventral prostate and v-Src prostate tumors. (F) The relative staining of the Trop2 ICD in the v-Src prostate tumors was increased 2-fold compared to non-transformed murine prostate gland. (G) The induction of Trop2 abundance assessed by Western blot in a series of v-Src PEC induced tumors. (H) The relative mRNA abundance of Trop2 and several other genes associated with the cancer stem cell in v-Src tumors and normal murine prostate.

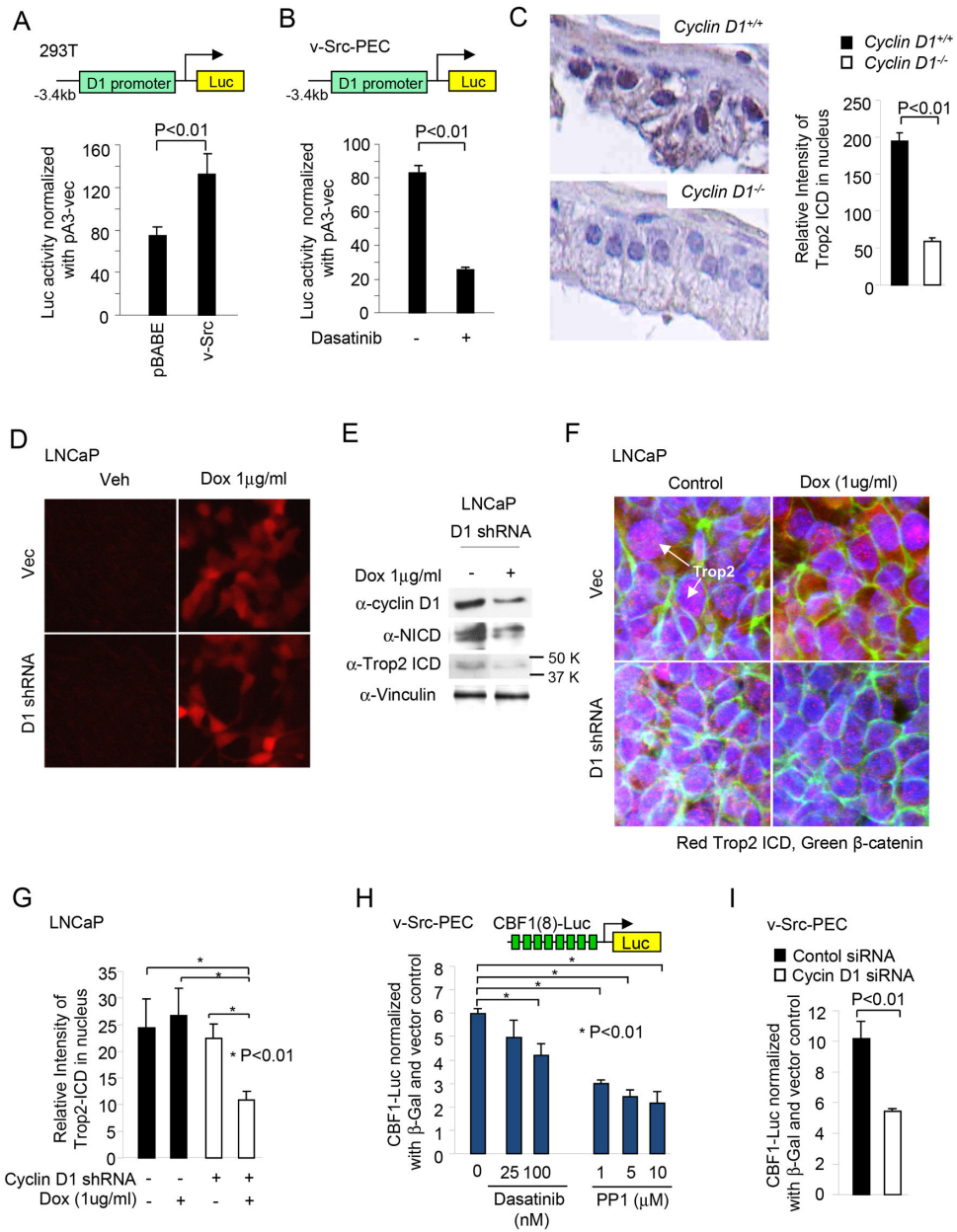


Figure 5. Cyclin D1 is required for v-Src induced Trop2 ICD

(A) -3,400bp cyclin D1-Luc activity was induced ~2-fold by v-Src in 293T cells, and (B) reduced 80% by Dasatinib in v-Src PEC cells. (C) The nuclear abundance of the Trop2 ICD is reduced in the *cyclin D1*^{-/-} prostate epithelium compared to *cyclin D1*^{+/+}. (D) Cyclin D1 shRNA induced by doxycycline in LNCaP cell with (E) Western blot analysis demonstrating the reduction in cyclin D1 abundance associated with a decrease in the Trop2 ICD. Vinculin is a protein loading control. (F-G) In cyclin D1 shRNA-treated LNCaP cells, the Trop2 ICD was reduced, shown by immunofluorescence staining (H) The Src Kinase inhibitors Dasatinib and PP1 reduced CBF activity in a dose-dependent manner in v-Src PEC. (I) CBF-Luc activity activity is shown in cyclin D1 siRNA-treated v-Src PEC cells.

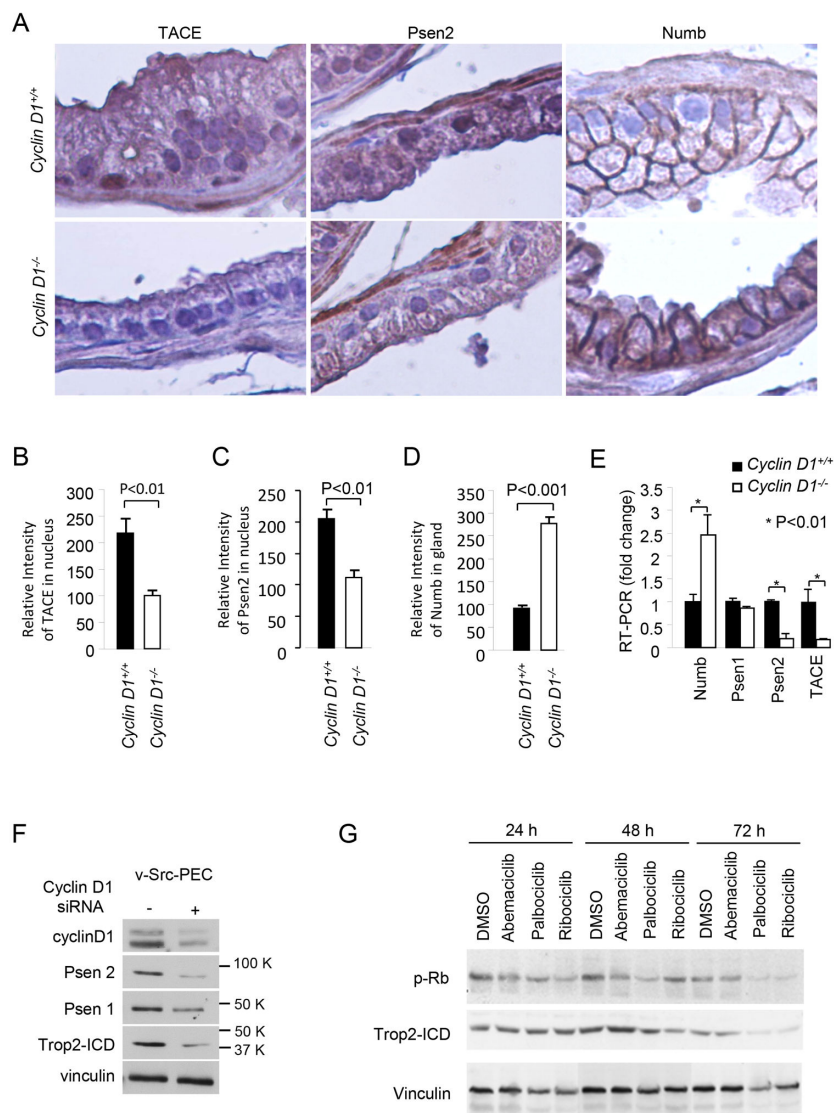


Figure 6. Cyclin D1 induces expression of the Trop2 cleavage complex
 (A) IHC staining of *cyclin D1*^{+/+} and *cyclin D1*^{-/-} mouse prostate glands. (B) The deletion of *cyclin D1* induced Numb abundance, reduced TACE (C) and PS2 (D) by ~50%. (E) RT-PCR demonstrating cyclin D1 reduced Numb and increased PS2 and TACE *in vivo*. (F) Western blot for v-Src cells transduced with cyclin D1 siRNA. The reduction in cyclin D1 abundance correlated with a reduction in Trop2 ICD. (G) The effects of the CDK inhibitor Abemaciclib, Palbociclib and Ribociclib on Trop2 ICD cleavage. CDK inhibitors decreased Trop2 ICD abundance after the 2nd day of CDK inhibitor treatment.

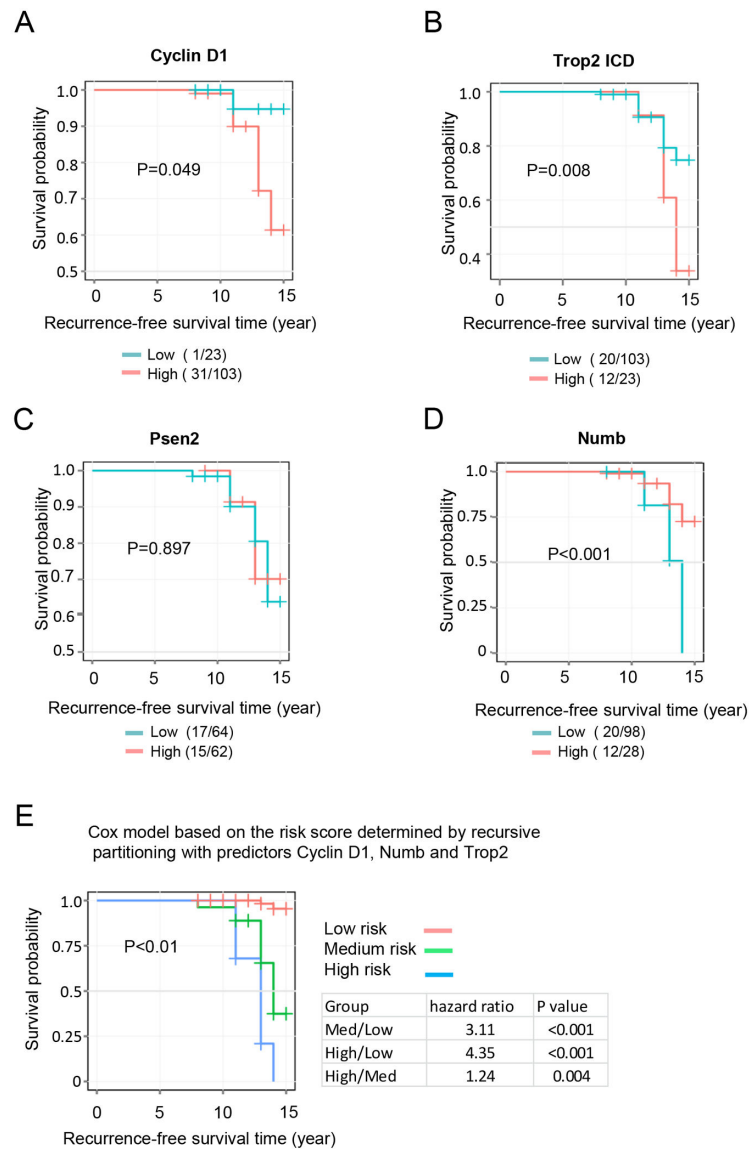


Figure 7. Recurrence-free survival analysis

Kaplan Meier analysis was used to evaluate the difference in recurrence-free survival associated with high expression versus low expression of Trop2 , (A) cyclin D1, B) Numb C), PS2 and D) Trop2 ICD. E) Combined the three target genes, patients were assigned to high, medium, low recurrence risk groups, the recurrence free survival curves of different groups and hazard ratio between groups are shown.